*Journal of the Geological Society, London*, Vol. **160**, 2003, pp. 271–284. Printed in Great Britain.

# Mid-Triassic integrated U–Pb geochronology and ammonoid biochronology from the Balaton Highland (Hungary)

JÓZSEF PÁLFY[1], RANDALL R. PARRISH[2,3], KARINE DAVID[2,4] & ATTILA VÖRÖS[1]

[1]*Department of Geology and Palaeontology, Hungarian Natural History Museum, POB 137, Budapest, H-1431 Hungary (e-mail: palfy@paleo.nhmus.hu)*

[2]*NERC Isotope Geosciences Laboratory, Kingsley Durham Centre, Keyworth NG12 5GG, UK*

[3]*Department of Geology, University of Leicester, Leicester LE1 7RH, Leicester, UK*

[4]*Present address: Laboratoire Magmas et Volcans, CNRS UMR 6524, 5, rue Kessler 63038, Clermont-Ferrand, France*

**Abstract:** Ladinian (Middle Triassic) strata of the Balaton Highland (west–central Hungary) comprise interbedded marine carbonate and volcaniclastic rocks. The sediments are noted for their rich ammonoid faunas, which allow detailed biostratigraphic subdivision and correlation. For the first time, isotopic dating of the tuff layers was carried out to calibrate the age of ammonoid zones and subzones. Four successive horizons were dated from the Felsőörs section, a candidate stratotype for the base of the Ladinian stage. Within the Reitzi Zone, which is interpreted here as the basal Ladinian unit, the following biostratigraphically tightly constrained U–Pb zircon ages were obtained: Felsoeoersensis Subzone 241.1 ± 0.5 Ma; Liepoldti Subzone 241.2 ± 0.4 Ma; Reitzi Subzone 240.5 ± 0.5 and 240.4 ± 0.4 Ma. A redeposited tuff from the Gredleri Zone at Litér yielded an additional U–Pb age of 238.7 ± 0.6 Ma. The new isotopic ages are in agreement with published U–Pb dates from the Southern Alps. Together, they allow estimation of the start of the Ladinian at 241.5 Ma and of the end of the stage at 237 Ma. A duration of <5 Ma for the stage strengthens the argument that cyclicity of the Ladinian Latemar platform (Southern Alps) is not exclusively of Milankovitch origin but forcing with shorter, sub-Milankovitch periods was also involved. The Ladinian, which started 10 Ma after the latest-Permian mass extinction, was a time of radiation and rapid evolutionary turnover, hence empirically established ammonoid biozones are of short duration, averaging 0.75 Ma.

**Keywords:** Middle Triassic, U–Pb geochronology, biochronology, time scale.

Isotopic dating using the U–Pb or $^{40}Ar/^{39}Ar$ method on volcaniclastic rocks intercalated within fossiliferous marine sediments offers the best means of time-scale calibration. For the Triassic time scale, recent studies constrained the period boundaries (Bowring *et al*. 1998; Pálfy *et al*. 2000a; Mundil *et al*. 2001), but reliable isotopic age determinations within the period remain scarce. The only exception is a set of U–Pb ages obtained by Mundil *et al*. (1996) from Ladinian volcaniclastic rocks interbedded in the pelagic successions of the Southern Alps in Italy and Switzerland. These dates are in conflict with earlier K–Ar ages of the same rocks (Hellmann & Lippolt 1981) and hence require a revision of the Anisian–Ladinian boundary age estimates given in recent time scales (Gradstein *et al*. 1994; Remane 2000). The ages reported by Mundil *et al*. (1996) are also at odds with cyclostratigraphic interval dating of the correlative Latemar carbonate platform (Goldhammer *et al*. 1987; Hinnov & Goldhammer 1991). The isotopic dates suggest that the >700 m thick sequence of carbonates on the Latemar platform was deposited in less than 5 Ma (Brack *et al*. 1996; Mundil *et al*. 1996), whereas Milankovitch-based estimates require 12 Ma (Goldhammer *et al*. 1987; Hinnov & Goldhammer 1991). Although recent cyclostratigraphic studies question the reliability of the U–Pb dating (Hardie & Hinnov 1997; Preto *et al*. 2001), an alternative interpretation of cyclicity through sub-Milankovitch forcing was also proposed (Schwarzacher 1998) and the controversy has remained unresolved. Consequently, testing the validity of the ages obtained by Mundil *et al*. (1996) is of considerable interest. One such test, independent dating of correlative volcaniclastic rocks, is presented here.

We report five new U–Pb dates from the Middle Triassic sequence of the Balaton Highland in Hungary, from stratigraphic levels that can be readily correlated with the isotopically dated successions in the Southern Alps. Pelsonia, a tectonostratigraphic terrane that includes the Balaton Highland (Kovács *et al*. 2000), has close affinities to the Southern Alps and the two regions were probably adjacent during Mid-Triassic time (Vörös 2000). Therefore the dated rocks derived from similar if not the same volcanic centres and their zircon systematics are expected to show similar behaviour and complexity.

The Balaton Highland is a classical area of Middle Triassic stratigraphy, which contributed to the early development of the ammonoid biostratigraphic scale (Böckh 1873; Mojsisovics 1882) and where continuing work resulted in a modern revision of zonal ammonoid biochronology (Vörös 1998). Four of the new isotopic dates were obtained from the Felsőörs section, a candidate Global Stratotype Section and Point (GSSP) for the Anisian–Ladinian stage boundary (Vörös *et al*. 1996) and the type locality of the Reitzi Zone (Vörös 1993), where its subzonal sequence is well established (Vörös 1998). The remarkably high resolution of the ammonoid biochronology is underpinned by high evolutionary turnover rate, possibly a feature of the diversity surge following a lengthy interval of suppressed diversity after the latest-Permian mass extinction. A refined Mid-Triassic time scale helps understand changes in the evolutionary tempo in this important interval in the history of life.

The principal goals of this study are the following: (1) to establish a numerically calibrated bio- and chronostratigraphic framework for the Felsőörs section; (2) to provide new calibra-

tion points for the Triassic time scale; (3) to compare our new dates with those of Mundil *et al*. (1996), so as to evaluate competing hypotheses on the cyclic origin of Mid-Triassic carbonate platforms in the Southern Alps; (4) to gauge the tempo of ammonoid evolution through estimation of the duration of the Reitzi Zone and its subzones; (5) to assess the trajectory of biodiversity changes following the latest-Permian mass extinction.

## Geological setting, localities and previous work

The Balaton Highland is a chain of rolling hills north of Lake Balaton and south of the Veszprém Plateau, rising some 200 m above the lake level. The Balaton Highland forms the southern flank of the Transdanubian Range, which is underlain by gently north-dipping Palaeozoic and Mesozoic strata (Fig. 1). The Triassic stratigraphy and sedimentary evolution of the area are summarized here after Balogh (1981), Haas & Budai (1995, 1999), Haas *et al*. (1995) and Vörös (2000). A schematic litho- and biostratigraphy, with correlation among the key sections, is shown in Figure 2. Slow transgression during earliest Triassic time deposited a shallow marine siliciclastic–carbonate series ('Werfen Group'), overlain by lower to middle Anisian carbonates of shallow marine ramp facies (including the Megyehegy Dolomite). This broad, uniform ramp was fragmented by synsedimentary extensional tectonic movements that started in mid-Anisian time. Carbonate platforms developed locally (Tagyon Limestone and Dolomite), whereas deeper-water carbonates (Felsőörs Limestone) were deposited in the intervening basins. Crustal thinning and disintegration of the margin was the result of rifting, which is also marked by traces of submarine volcanism starting near the Anisian–Ladinian boundary ('pietra verde' tuffs). In the Ladinian, a pattern of relatively deep basins with

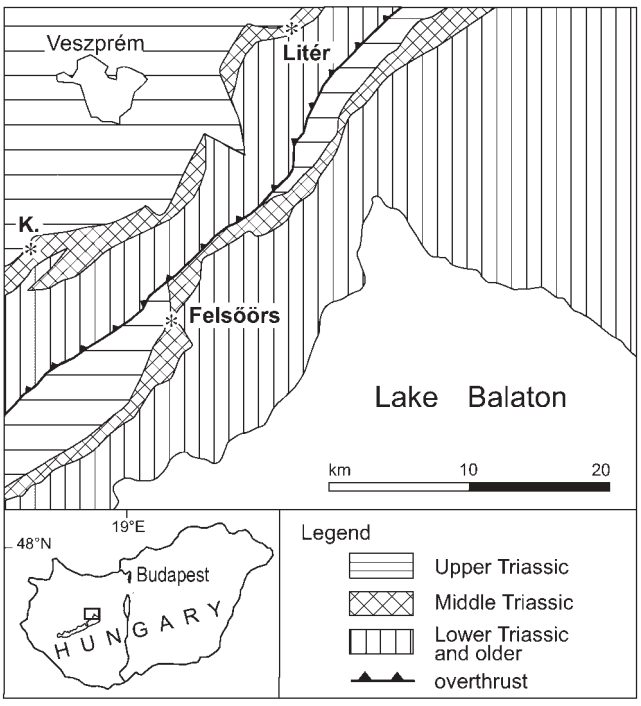


**Fig. 1.** Location of the studied sections on a simplified geological map of the northeastern Balaton Highland and the Veszprém Plateau. K., Katrabóca.

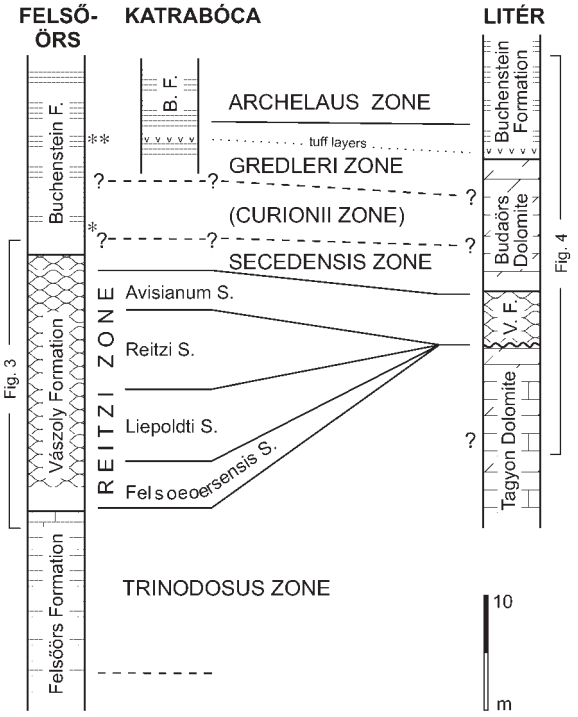


**Fig. 2.** Overview of bio- and lithostratigraphy and correlation of the studied sections from the Middle Triassic sequence of the Balaton Highland. B.F., Buchenstein Formation; V.F., Vászoly Formation; *, occurrence of *Eoprotrachyceras* cf. *curionii;* **, occurrence of *Arpadites*?.

pelagic, cherty carbonates (Buchenstein Formation) and surviving platforms, with 500–1000 m thick peritidal carbonate sequences (Budaörs Dolomite) was established. During the Carnian, the influx of fine terrigenous clastic material partly infilled the basins. The top of the Triassic system is represented by a Norian to Rhaetian dolomite and limestone complex of >1 km thickness ('Hauptdolomit' and Dachstein Limestone).

The Balaton Highland, together with the entire Transdanubian Range, is part of a large tectonostratigraphic terrane called Pelsonia (Kovács *et al*. 2000). In the early Mesozoic, this terrane belonged to the wide carbonate shelf margin of the western Tethys and was in close proximity to the Southern Alps (Kázmér & Kovács 1985; Haas *et al*. 1995; Vörös 2000). A palaeogeographical reconstruction of facies belts allows the placement of the Balaton–Bakony zone of Pelsonia adjacent to the East Lombardy–Giudicarie–Dolomites segment of the Southern Alps (Budai & Vörös 1993; Haas & Budai 1995; Vörös & Galácz 1998).

The Mid-Triassic tectonosedimentary evolution of the Balaton Highland was described in detail by Budai & Vörös (1992, 1993) and Vörös *et al*. (1997), whereas analogies to the Southern Alps were discussed by Budai (1992) and Haas & Budai (1995). The Anisian platform carbonate (Megyehegy Dolomite) and basin facies (Felsőörs Limestone) have their Southern Alpine equivalents in the Dosso dei Morti and Upper Serla Formations, and the Prezzo Limestone, respectively. The Buchenstein Formation refers to analogous sequences in both regions (including the Livinallongo Formation of the Dolomites). The Budaörs Dolomite may correspond to the Latemar–Sciliar platform carbonates in the Southern Alps. The Mid-Triassic, rift-related tectonic differentiation is common to both regions and is related to the onset of volcanism.

The volume, distribution and lithology of this volcanism, however, shows considerable differences between the two areas (Castellarin *et al*. 1980; Pisa *et al*. 1980; Cros & Szabó 1984; Budai & Vörös 1993). The lowermost significant tuff layers in the lower Buchenstein beds (Reitzi Zone; 'Reitzi tuffs') are much thicker (attaining 8–10 m) in the Balaton Highland than anywhere in the Southern Alps. Higher in the lower Ladinian sequence, this relationship is reversed as the thickness of tuff layers increases in the Southern Alps, whereas the thin tuffaceous intercalations become rare between the cherty limestone beds in the Balaton Highland. Thick lava flows and complex pyroclastic and volcaniclastic rocks produced by late Ladinian volcanic eruptions in the Southern Alps (Wengen beds) have no counterparts in the Balaton Highland basin, where only thin tuff layers occur (e.g. at Katrabóca, Vörös 1998). Only in the eastern Bakony Mts are the products of the late Ladinian volcanism more voluminous, but the stratigraphical relationships of this >20 m thick volcaniclastic formation are not clear (Budai *et al*. 2001b). A common feature of the Ladinian volcanism in the Balaton Highland and the Southern Alps is the geochemical transition from early Ladinian acidic to late Ladinian intermediate or basic composition.

The early Ladinian explosive acidic volcanism with unidentified (presumably not preserved) eruption centres produced several tuff levels that are widespread in both regions. These tuffs are tightly constrained by ammonoid biostratigraphy of the adjacent sediments and their age constitutes the main subject of this paper.

### *The Felsőörs section*

Four samples were collected for U–Pb dating from the Middle Triassic section at Felsőörs (Fig. 3). The locality, also known as Forrás Hill or Malom Valley, is easily accessible as it lies only 200 m NW of the village of Felsőörs. The lower part of the section consists of natural outcrops at the hillside, whereas the higher, more fossiliferous strata are exposed by artificial trenches. The section was recently re-excavated and it is now a protected geological heritage site.

The fossiliferous beds at Felsőörs have been studied for over 130 years. Roth (1871), Böckh (1873) and Stürzenbaum (1875) carried out the first bed-by-bed collections and described some distinctive ammonoids from the 'yellow, siliceous limestones of Forrás Hill'. The definition by Mojsisovics (1882) of his 'Zone des Trachyceras Reitzi' was largely based on the findings at Felsőörs. The first modern descriptions of the section and some new data on its microfauna were given by Szabó *et al*. (1980). Subsequent, integrated ammonoid, conodont and radiolarian biostratigraphic studies amply documented that the Felsőörs section straddles the Anisian–Ladinian boundary, thus it was proposed as a candidate Global Stratotype Section and Point (GSSP) for the base of the Ladinian stage (Vörös *et al*. 1996). During the prolonged debate over the boundary problem, further results on integrated magnetostratigraphy (Márton *et al*. 1997) and ammonoid biostratigraphy (Vörös 1998) were published, and additional palaeomagnetic measurements are in progress.

The basal unit of the Middle Anisian to Upper Ladinian sequence is the thick-bedded dolomicrosparite of the Megyehegy Formation. Higher in the sequence, bituminous, thin-bedded dolomitic limestone and marl of restricted basin facies are overlain by limestone with chert nodules and crinoidal–brachiopodal marly limestone of the Felsőörs Formation. Still higher, the grey limestone includes a tuff horizon and clayey interbeds. The higher part of the Felsőörs Formation belongs to the Trinodosus Zone, subdivided here into the Trinodosus, Camunum and Pseudohungaricum subzones (Vörös *et al*. 1996).

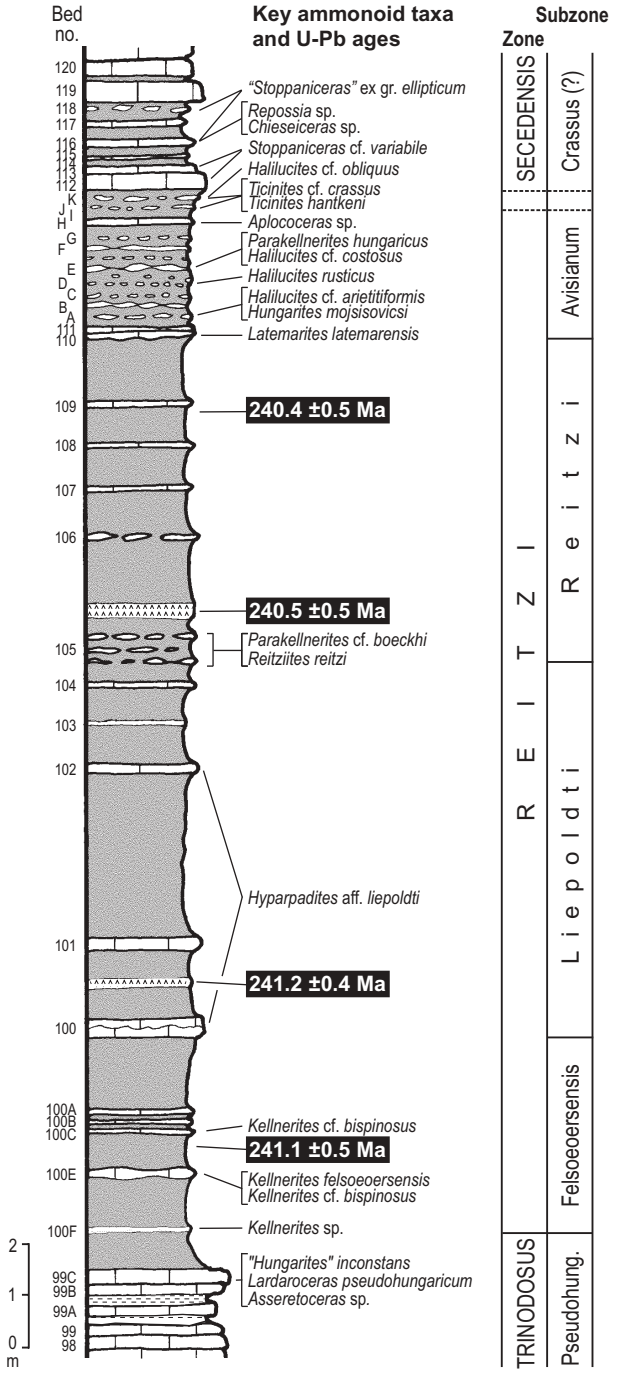


**Fig. 3.** Measured stratigraphic section at Forrás Hill near Felsőörs, showing the biostratigraphic subdivision based on occurrences of age diagnostic ammonoid taxa, and the U–Pb ages of dated tuff layers.

The overlying tuffaceous succession of the Vászoly Formation begins at the top of Bed 99/C (Fig. 3). The lower, 18 m thick part of this sequence consists of potassium-trachyte tuff, with interbedded, locally lenticular limestone. The occurrence of zircon in the tuff layers was noted by Dunkl (1992), who determined fission-track ages between 210 and 260 Ma. In the

higher part of the Vászoly Formation, carbonate sedimentation is resumed as nodular limestone predominates over tuffaceous clay. These beds were previously interpreted as debris flows (Kovács 1993; Vörös *et al*. 1996) but repeated sampling disproved this because the continuous or flaser-bedded limestone layers contain an ordinary succession of ammonoid assemblages. The ammonoid succession within the Vászoly Formation, assigned to the Reitzi and Secedensis zones, is discussed in detail below.

The volcanic ash component decreases upsection, giving way to a thick, continuous sequence of red, cherty limestone. This pelagic, basinal limestone of the Buchenstein Formation is poorly exposed and no detailed collection of ammonoids was made from this formation. A fragment of *Eoprotrachyceras* cf. *curionii* and, higher, a few poorly preserved fragments of *Arpadites* sp. were found in the scree, suggesting the presence of the Curionii and the Gredleri zones, respectively.

### *The Litér quarry*

An additional U–Pb age was obtained from a sample collected from the Litér dolomite quarry, which lies between the village of Litér and Highway 8. The Anisian to Upper Ladinian section, described in detail by Budai *et al*. (2001a), is exposed in the western, abandoned part of the quarry. The massive Tagyon Dolomite of late? Anisian age is unconformably overlain by the Vászoly Formation dipping at 30° to the north. The crinoidal limestone layers and tuffaceous interbeds represent the Avisianum Subzone of the Reitzi Zone (Vörös 1998). Upsection, a 10 m thick, massive dolomite body, a tongue of the prograding Budaörs Dolomite, is overlain by nodular, siliceous limestone of the Buchenstein Formation (Fig. 4). Its lowermost beds contain tuffaceous clay and marl intercalations and provided numerous Arcestidae ammonoids and a specimen of *Protrachyceras* cf. *gredleri*, indicating the Gredleri Zone. Higher up, a large specimen of *Protrachyceras ladinum* was found in the scree, suggesting the presence of the Archelaus Zone.

In the southern corner of the quarry, the Tagyon Dolomite is exposed at the surface. It is penetrated by a 1 m wide, nearly vertical fissure filled with a mixture of tuff and lithoclasts that comprise mud pebbles and internal moulds of ammonoids. A poorly preserved but abundant ammonoid fauna consists of *Protrachyceras* cf. *gredleri* (Fig. 5h), *P.* cf. *longobardicum* (Fig. 5i), *Eoprotrachyceras*? cf. *pseudoarchelaus* and *Arpadites* cf. *arpadis* (Fig. 5j). This assemblage indicates the upper part of the Gredleri and lower part of the Archelaus zones. Some specimens are worn internal moulds, suggesting redeposition and transport from unconsolidated mudstones, whereas others are filled with tuff, suggesting that their embedding was synchronous with the deposition of volcanic ash.

The fissure is interpreted as a neptunian dyke that opened at the beginning of the Archelaus Zone. At the time of its abrupt opening, layers of unconsolidated lime mud and ash were already deposited on the dolomite surface. The infilling was probably a short episode. The semi-consolidated lime mud layers easily disintegrated and mud clasts together with sediment-laden ammonoid shells were carried by gravity sliding into the fissure (Fig. 4). The water-saturated, possibly liquefied volcanic ash was volumetrically dominant and composed the matrix of the fissure fill. The lime mud layers, eventually redeposited into the fissure, spanned the uppermost Gredleri to lowermost Archelaus zones.

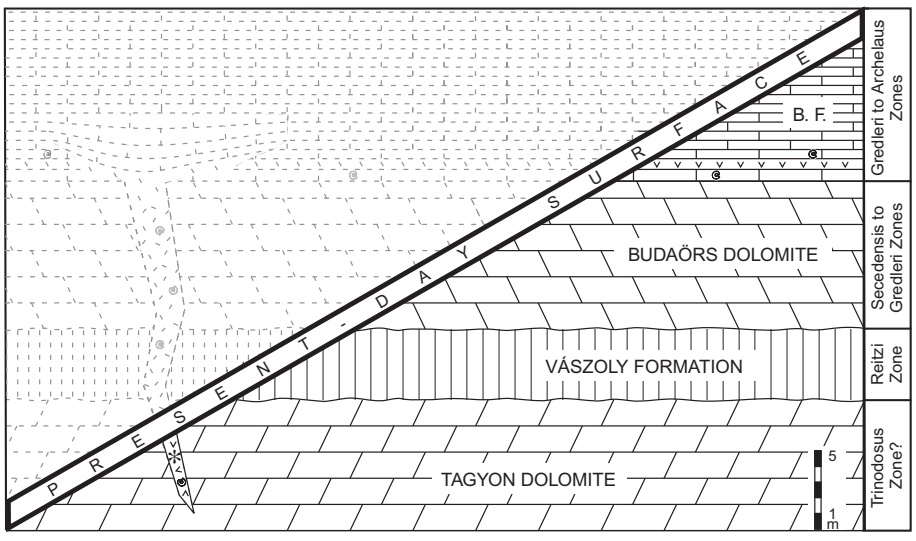


**Fig. 4.** Bio- and lithostratigraphy of the Litér quarry, with an interpretive genetic model of the neptunian dyke sampled for U–Pb dating. Dashed lines indicate rocks removed by erosion. (Note that present-day dip of strata is 30°.)

**Fig. 5.** Age diagnostic ammonoids from the Felsőörs and Litér sections. All specimens are natural size and deposited in the Department of Geology and Palaeontology of the Hungarian Natural History Museum (Budapest); under the inventory numbers prefixed with M. (**a**) *Kellnerites felsoeoersensis* (Stürzenbaum), M.98.6, Reitzi Zone, Felsoeoersensis Subzone, Vászoly Formation, Felsőörs, Bed 100/E. (**b**) *Lardaroceras* aff. *pseudohungaricum* Balini, M.2001.26, Reitzi Zone, Felsoeoersensis Subzone, Vászoly Formation, Felsőörs, Bed 100/E. (**c**) *Reitziites reitzi* (Böckh), M.2001.27, Reitzi Zone, Reitzi Subzone, Vászoly Formation, Felsőörs, Bed 105. (**d**) *Hyparpadites* aff. *liepoldti* (Mojsisovics), M.98.22, Reitzi Zone, Liepoldti Subzone, Vászoly Formation, Felsőörs, Bed 102. (**e**) *Parakellnerites boeckhi* (Roth), M.98.28, Reitzi Zone, Reitzi Subzone, Vászoly Formation, Felsőörs, Bed 105. (**f**) *Latemarites latemarensis* Brack & Rieber, M.2001.28, Reitzi Zone, Avisianum Subzone, Vászoly Formation, Felsőörs, Bed 110/111. (**g**) *Latemarites latemarensis* Brack & Rieber, M.2001.29, Reitzi Zone, Avisianum Subzone, Vászoly Formation, Felsőörs, Bed 110/111. (**h**) *Protrachyceras* cf. *gredleri* (Mojsisovics), M.98.55, Gredleri–Archelaus Zone, Buchenstein Formation (?), Litér quarry, neptunian dyke. (**i**) *Protrachyceras* cf. *longobardicum* (Mojsisovics), M.98.112, Gredleri–Archelaus Zone, Buchenstein Formation (?), Litér quarry, neptunian dyke. (**j**) *Arpadites* cf. *arpadis* (Mojsisovics) (M.98.50), Gredleri–Archelaus Zone, Buchenstein Formation (?), Litér quarry, neptunian dyke.

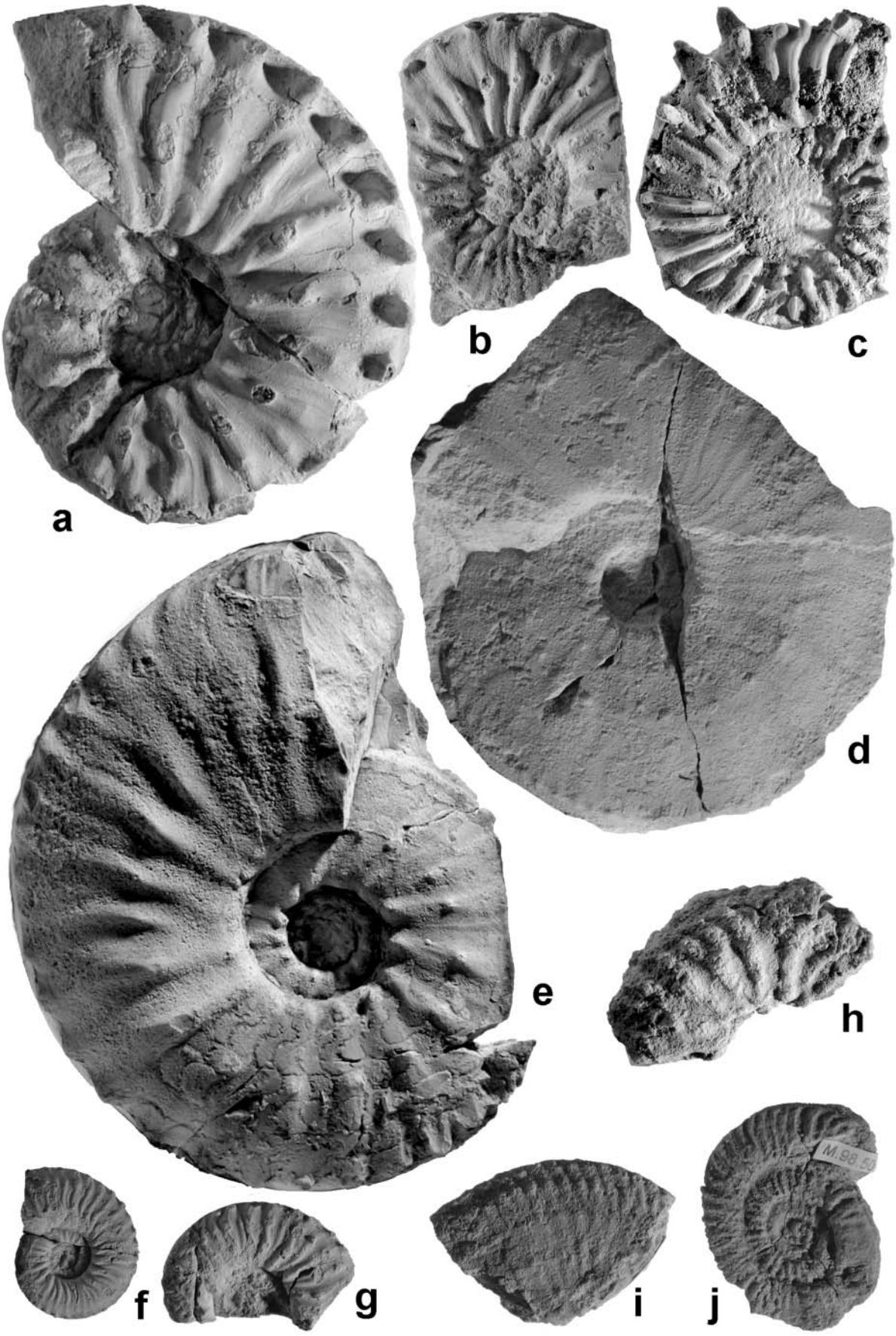
a
b
c
d
e
f
g
h
i
j

Two lines of evidence suggest that the ash was confined to the uppermost part of the Gredleri Zone: one specimen of *P. gredleri* is filled with tuff; and at Katrabóca, the only well-studied upper Ladinian section in the Balaton Highland (Vörös 1998), there are three thin tuffaceous horizons in the upper part of the Gredleri Zone, whereas no traces of tuff are found in the lower Archelaus Zone. Therefore we correlate the ash-fall episode recorded at Katrabóca with that represented by the tuff filling the neptunian dyke of Litér (Fig. 2).

## Ammonoid biochronological subdivision and correlation

To provide biochronological constraints for the new U–Pb ages, here we discuss the ammonoid zonation scheme used, establish the biostratigraphic subdivisions in the studied sections, and outline their correlation with other areas, chiefly with the Southern Alps from where a comparably detailed faunal record and isotopic ages exist.

The boundaries and subdivision of the Ladinian stage are widely debated (Brack & Rieber 1993, 1994; Mietto & Manfrin 1995; Vörös *et al*. 1996). At present no international agreement exists about the preferred position and site of the GSSP for the base of the stage. Currently there are three formal proposals for the position of the base of Ladinian: (1) at the first appearance of *Kellnerites*, i.e. at the base of the Reitzi Zone; (2) at the first appearance of *Nevadites*, i.e. at the base of the Secedensis Zone; (3) at the first appearance of *Eoprotrachyceras*, i.e. at the base of the Curionii Zone. A fourth option, at the first appearance of *Reitziites*, i.e. at the base of the Reitzi Subzone, was also suggested (Kozur *et al*. 1995), whereas a quantitative biostratigraphic study using the unitary association method concluded that the base of the Avisianum Subzone is marked by the most pronounced ammonoid turnover event in the interval in question, hence it may offer the best correlation potential as the base of Ladinian (Pálfy & Vörös 1998). Biostratigraphic units discussed in the text are shown in Figure 2. In the present paper, we follow the ammonoid zonal scheme proposed by Brack & Rieber (1993), that was also used by Mundil *et al*. (1996) and slightly modified by Vörös *et al*. (1996). A significant difference is that we regard the Reitzi Zone as the basal unit of the Ladinian but this has no effect on the correlation. The Reitzi Zone is not only the best studied interval at the Anisian–Ladian transition, but also it has the finest subdivision and allows the most reliable biostratigraphic correlation between the Balaton Highland and the Southern Alps (especially the Bagolino section) at the subzone level (Vörös *et al*. 1996).

The lower boundary of the Felsoeoersensis Subzone, and the Reitzi Zone itself, is marked by the first appearance of the genus *Kellnerites* (Fig. 5a). The fauna is characterized by various, perhaps partly synonymous species of *Kellnerites*, together with *Hungarites*, and a form close to *Parakellnerites*, which is herein referred to as *Lardaroceras*? aff. *pseudohungaricum* (Fig. 5b). The subzone comprises Beds 100F–100A at Felsőörs, which correspond to the 53.0–55.5 m interval in Bagolino and parts of the Pertica section.

The faunal assemblage of the Liepoldti Subzone is less diverse than that of the adjacent subzones. The only characteristic element is the genus *Hyparpadites*, represented by *H. liepoldti*, *H*. aff. *liepoldti* (Fig. 5d) and *H. bagolinensis* (= *Kellnerites bagolinensis* of Brack & Rieber 1993, 1994). Beds 100–104 at Felsőörs are assigned to the subzone and correlated with the interval 55.5–56.5 m in the Bagolino section and parts of the Pertica section.

The base of the Reitzi Subzone is well defined in several sections of the Balaton area (e.g. at Bed 105 in Felsőörs) and also in the Southern Alps at Bagolino (at 56.5 m) by the first appearance of *Reitziites reitzi* (Fig. 5c) and other, perhaps synonymous species of the same genus, accompanied by *Parakellnerites boeckhi* and *Hungarites*.

The Avisianum Subzone is well represented in the Balaton Highland (Vörös 1998) and is the most widespread subzone of the Reitzi Zone in the Southern Alps (De Zanche *et al*. 1995). Its rich fauna is characterized by *Aplococeras*, *Latemarites*, several species of *Halilucites* and peak abundance of the genus *Parakellnerites*. At Felsőörs, the limestone Beds 110 and/or 111 contain *Latemarites latemarensis* (Fig. 5f–g) (collected earlier by L. Krystyn) that marks the base of the Avisianum Subzone. The overlying Beds 111/A–111/K yielded a rich and diverse ammonoid fauna, with a *Ticinites* horizon occurring at the top of the subzone. The lower boundary of the Avisianum Subzone is not well defined in Bagolino, whereas in M. San Giorgio it is drawn at Bed 41. Some of the Southern Alpine sections studied by Mietto & Manfrin (1995) (e.g. Punta Zonia) may help better define the base of this subzone.

Bed 112 at Felsőörs yielded *Stoppaniceras* cf. *variabile*, whereas *Chieseiceras*, *Repossia* and '*Stoppaniceras*' ex. gr. *ellipticum* occur in the limestone layers in the overlying tuffaceous clay. This assemblage represents the Secedensis Zone.

Four of the tuff layers that we dated isotopically belong to the Reitzi Zone, thus it is important to emphasize that their biostratigraphic constraints are tight and correlation with the Southern Alpine sections is well founded. Tracing of individual tuff layers across these distant areas is tenuous but not impossible. We postulate that the tuff horizon at Felsőörs sampled as F101 corresponds to the $T_a$ tuff layer in Bagolino, whereas a tuff yielding sample F105 can be correlated with one of two higher tuff layers in the Reitzi Zone, below tuff layer $T_b$ at Bagolino (see Brack & Rieber 1993).

The biostratigraphic constraints and correlation of the higher Ladinian tuffs in the Balaton Highland and the Southern Alps (Bagolino, Seceda) are less clear. No detailed biostratigraphic subdivision exists for the higher Curionii, Gredleri and Archelaus ammonoid zones (Krystyn 1983) and their correlation within the Alpine–Tethyan region is more problematic than for the Reitzi and Secedensis zones. The taxonomy and stratigraphic ranges of the ammonoid fauna from Epidaurus in Greece, where Krystyn (1983) established the Gredleri Zone, are poorly known or not published. The late Ladinian faunas of the Southern Alps are partly published but the record is rather incomplete and the zonal schemes of different workers (Brack & Rieber 1993; Fantini Sestini 1994; Mietto & Manfrin 1995) are controversial. Only Mietto & Manfrin (1995) developed a formal zonal and subzonal subdivision for the late Ladinian but this was criticized and not applied by Balini *et al*. (2000). Bed-by-bed collections at Katrabóca helped clarify drawing the Gredleri–Archelaus zonal boundary (Vörös 1998). It appears practical to characterize the upper part of the Gredleri Zone by the co-occurrence of *Protrachyceras gredleri* and abundant and diverse species of *Arpadites*, whereas the base of the Archelaus Zone is best marked by the almost synchronous appearance of *P. ladinum*, *P. longobardicum* and *P. archelaus* (Vörös 1998). Our own examination of L. Krystyn's collection from Epidaurus also justifies this practice.

Difference between this interpretation of the base of the Archelaus Zone and that of Brack & Rieber (1993) is of importance for the present study. Both Brack & Rieber (1993) and Mundil *et al*. (1996) placed a U–Pb dated tuff horizon at Bagolino, sampled as BAG.06a, into the lower part of the

Gredleri Zone. Although the occurrence of *Arpadites arpadis* immediately above the tuff confirms this zonal assignment, only 1 m higher is the first appearance of *Protrachyceras* cf. *longobardicum*, which, in our opinion, marks the base of the Archelaus Zone. Thus the tuff BAG.06a belongs to the higher part of the Gredleri Zone, and consequently it is correlated with the tuff horizons at Katrabóca (Vörös 1998) and Litér (Budai *et al*. 2001a, this study).

## Integrated bio- and geochronology

### *U–Pb zircon analytical methods*

All U–Pb age determinations reported here were performed at the NERC Isotope Geosciences Laboratory of the British Geological Survey in Keyworth. Approximately 15–20 kg samples were collected with care to avoid contamination by zircons from other samples in both the field and laboratory. Zircons were separated and purified using a mixture of mechanical crushing, sieving using disposable screens, vibration on a Rogers wet shaking table, panning, heavy liquids and Frantz model LB-1 magnetic separation techniques. Zircon crystals that were clear and crack-free were selected for further processing, after careful high-magnification observation for potential xenocryst cores. Moderate to strong air abrasion with pyrite using the method of Krogh (1982) was applied to remove *c*. 10–30% of the mass of the grains, with the aim of removing all crystallographic external surfaces. Abraded grains were leached in warm 10% $HNO_3$ to remove residual pyrite. Further selection of grains into groups of similar size and shape preceded analysis.

Leaching in warm 3N $HNO_3$ in the clean chemistry laboratory was followed by loading into TFE Teflon capsules (Parrish 1987), addition of a $^{205}Pb$–$^{230}Th$–$^{233}U$–$^{235}U$ or $^{205}Pb$–$^{235}U$ mixed tracer calibrated against a gravimetric U–Th–Pb solution, addition of HF–$HNO_3$ acid and dissolution at 240 °C for 36–48 h. Because the verification of complete dissolution that is necessary for thorough sample–tracer homogenization cannot be ensured using observation in Teflon vessels or in ordinary laboratory lighting conditions, our solutions were checked for zircon dissolution by pouring the zircon and tracer solution into a pre-cleaned PMP clear beaker held under clean air conditions and brilliant fibre optic illumination. At 240 °C, complete dissolution is routinely observed for zircon. U and Pb separation and purification followed methods of Parrish *et al*. (1987). Mass spectrometer measurements were made on a VG354 instrument using an ion counting Daly photomultiplier, in part Faraday cups, and a WARP filter for high abundance sensitivity (Noble *et al*. 1993). Suitable corrections for mass fractionation and other minor effects have been made. The blanks for the procedure varied from 4 to 20 pg Pb and from 0 to 1 pg U, using numerous measurements made concurrently using the mixed spike mentioned above so that the full composition of the blanks could be recovered. Two sets of typical isotopic ratios of the blank are as follows: $^{206}Pb/^{204}Pb$ 18.77, $^{207}Pb/^{204}Pb$ 15.44, $^{208}Pb/^{204}Pb$ 37.6; and $^{206}Pb/^{204}Pb$ 17.69, $^{207}Pb/^{204}Pb$ 15.09, $^{208}Pb/^{204}Pb$ 36.67. The standard deviation of the blank composition is also used in the error propagation. Common Pb corrections above those of the laboratory blank were made using 241 Ma Pb according to the method of Stacey & Kramers (1975). Measurements of a solution of the 91500 zircon standard were also made during the study to monitor mass spectrometer and chemical procedure performance. Ages were calculated using constants determined by Jaffey *et al*. (1971), as recommended by Steiger & Jäger (1977). The errors have been propagated using the method of Parrish *et al*. (1987) and Roddick (1987). The interpretation of age has been assessed using the methods and algorithms of Ludwig (1998, 2000).

### *Age determinations*

The analytical results are presented in Table 1 and shown in Figures 6 and 7. Concordant multiple-grain analyses were duplicated for all five samples studied. These clusters of data were used in the calculation of both concordia ages and weighted means of the most precise $^{206}Pb/^{238}U$ ratio using methods outlined by Ludwig (1998). Final ages quoted below and in Table 2 include the uncertainty in the decay constant errors. In assessing the final ages, we make the assumption that crystals in the analysed fractions used in the final age calculations have not suffered from Pb loss or inheritance and that they have behaved as closed systems since crystallization. This assumption is consistent with the observation that the dispersion of data about the means for the 15 analyses used in the final age calculations are very close to what one would expect as a result of measurement uncertainty alone. If xenocryst grains of significantly older age were present in the multi-grain analyses, a greater degree of dispersion would probably be observed and the consistency with stratigraphic order would not necessarily be preserved. A more difficult problem is the possibility of minor Pb loss if it is not entirely eliminated by air abrasion. Theoretically, a bias towards slightly younger ages cannot be ruled out, if all fractions contained one or more crystals with subtle residual Pb loss after the air abrasion treatment.

*Sample F100.* Our stratigraphically lowest dated sample in the Felsőörs section was collected from a 2 cm thick, green crystal tuff layer that contains abundant feldspar, biotite and quartz grains up to 0.5 mm in size. The tuff lies 50 cm below limestone Bed 100D and immediately above Bed 100E. The underlying limestone bed yielded *Kellnerites felsoeoersensis* (Fig. 5a), *K*. cf. *bispinosus*, *K*.? sp. and *Lardaroceras*? aff. *pseudohungaricum* (Fig. 5b), which indicate the Felsoeoersensis Subzone. The sampled layer is near the base of the subzone, hence also near the base of the Reitzi Zone.

The sample yielded abundant, colourless zircons of excellent clarity and low U content (130–230 ppm). The euhedral grains form two morphologically homogeneous populations: short, doubly terminating prisms and needles of simple quadratic cross-section and length:width ratio of up to 10:1. Fractions 1 and 2 are discordant and probably contained inherited cores or older xenocrysts that were not detected during the visual selection of grains. The other four fractions (3–6) are concordant and overlapping around a weighted mean $^{206}Pb/^{238}U$ age of 241.0 ± 0.5 Ma (Fig. 6). We use their concordia age of 241.1 ± 0.5 Ma as the best estimate of the crystallization age of the tuff.

*Sample F101.* Located 3 m stratigraphically above sample F100 in the Felsőörs section, this sample was collected from a 10–12 cm thick brown crystal tuff. The layer is 70 cm above limestone Bed 100, which yielded *Hyparpadites* aff. *liepoldti* (Fig. 5d), and is therefore assigned to the base of the Liepoldti Subzone, in the lower part of the Reitzi Zone.

The sample yielded abundant, colourless to pale yellow zircons of excellent clarity and low U content (130–360 ppm). The morphology of euhedral grains ranges from subequant, multifaceted, doubly terminating prisms to needles of simple quadratic cross-section and length:width ratio of up to 8:1. Although all six analysed fractions intersect the concordia curve, the apparent age of fraction 1 at *c*. 246 Ma and that of fraction 4

**Table 1.** *U–Pb zircon analytical data*

| Analysis[1] (sample and fraction) | Weight (mg) | U (ppm) | Pb (ppm)[2] | $^{206}Pb/^{204}Pb$[3] | Pb (pg)[4] | Th/U[5] | $^{206}Pb/^{238}U$[6] | 1σ error (%) | $^{207}Pb/^{235}U$[6] | 1σ error (%) | $^{207}Pb/^{206}Pb$[6] | 1σ error (%) | $^{206}Pb/^{238}U$ age[6] | 2σ error[7] | $^{207}Pb/^{235}U$ age[6] | 2σ error[7] | $^{207}Pb/^{206}Pb$ age[6] | 2σ error[7] | Correlation coefficient |
|---|---|---|---|---|---|---|---|---|---|---|---|---|---|---|---|---|---|---|---|
| *F100* | | | | | | | | | | | | | | | | | | | |
| 1 (M,el,9) | 0.0836 | 138.2 | 5.857 | 3049 | 10 | 0.41 | 0.04166 | 0.21 | 0.2994 | 0.24 | 0.05212 | 0.11 | 263.1 | 1.1 | 265.9 | 1.1 | 290.6 | 5.0 | 0.89 |
| 2 (M,el,16) | 0.1057 | 174.4 | 12.98 | 6863 | 12 | 0.31 | 0.07239 | 0.20 | 0.9667 | 0.20 | 0.09686 | 0.05 | 450.5 | 1.7 | 686.8 | 2.0 | 1564.5 | 1.7 | 0.98 |
| 3 (S,n,13) | 0.1270 | 130.1 | 5.095 | 3472 | 11 | 0.46 | 0.03800 | 0.22 | 0.2675 | 0.24 | 0.05106 | 0.11 | 240.4 | 1.0 | 240.7 | 1.0 | 243.7 | 5.0 | 0.89 |
| 4 (M,el,n,27) | 0.0675 | 228.1 | 9.077 | 2812 | 13 | 0.51 | 0.03818 | 0.23 | 0.2685 | 0.27 | 0.05100 | 0.14 | 241.6 | 1.1 | 241.5 | 1.2 | 240.7 | 6.3 | 0.86 |
| 5 (M,el,t,19) | 0.0718 | 231.5 | 9.248 | 3001 | 13 | 0.53 | 0.03810 | 0.16 | 0.2690 | 0.20 | 0.05120 | 0.16 | 241.0 | 0.8 | 241.9 | 0.9 | 249.9 | 7.5 | 0.63 |
| 6 (M,eq,15) | 0.0647 | 196.4 | 7.823 | 2878 | 10 | 0.52 | 0.03806 | 0.26 | 0.2682 | 0.31 | 0.05110 | 0.17 | 240.8 | 1.2 | 241.2 | 1.3 | 245.6 | 7.8 | 0.84 |
| *F101* | | | | | | | | | | | | | | | | | | | |
| 1 (M,el,21) | 0.0843 | 206.7 | 8.275 | 5028 | 8 | 0.45 | 0.03898 | 0.11 | 0.275 | 0.13 | 0.05116 | 0.09 | 246.5 | 0.5 | 246.7 | 0.6 | 247.9 | 4.1 | 0.75 |
| 2 (L,el,12) | 0.1002 | 192.9 | 7.631 | 4464 | 10 | 0.49 | 0.03810 | 0.12 | 0.2688 | 0.14 | 0.05118 | 0.09 | 241.0 | 0.6 | 241.8 | 0.6 | 249.0 | 4.1 | 0.76 |
| 3 (M,eq,7) | 0.0560 | 129.4 | 5.077 | 1757 | 10 | 0.46 | 0.03812 | 0.11 | 0.2684 | 0.22 | 0.05106 | 0.18 | 241.2 | 0.5 | 241.4 | 0.9 | 243.6 | 8.1 | 0.58 |
| 4 (S,n,25) | 0.0820 | 325.9 | 12.75 | 4013 | 15 | 0.49 | 0.03775 | 0.15 | 0.2651 | 0.17 | 0.05092 | 0.10 | 238.9 | 0.7 | 238.8 | 0.7 | 237.4 | 4.5 | 0.83 |
| 5 (M,n,17) | 0.0922 | 362.3 | 14.17 | 4826 | 16 | 0.46 | 0.03798 | 0.26 | 0.2673 | 0.27 | 0.05103 | 0.10 | 240.3 | 1.2 | 240.5 | 1.2 | 242.1 | 4.6 | 0.93 |
| 6 (M,eq,10) | 0.0757 | 264.1 | 10.61 | 10160 | 5 | 0.55 | 0.03807 | 0.26 | 0.2684 | 0.27 | 0.05114 | 0.11 | 240.9 | 1.2 | 241.5 | 1.2 | 247.2 | 4.9 | 0.92 |
| *F105* | | | | | | | | | | | | | | | | | | | |
| 1 (L,el,14) | 0.1058 | 148.7 | 5.923 | 1538 | 25 | 0.43 | 0.03898 | 0.30 | 0.2792 | 0.34 | 0.05194 | 0.15 | 246.5 | 1.5 | 250.0 | 1.5 | 282.6 | 6.9 | 0.90 |
| 2 (M,n,16) | 0.0505 | 165.1 | 6.572 | 2845 | 5 | 0.54 | 0.03790 | 0.32 | 0.2670 | 0.34 | 0.05111 | 0.27 | 239.8 | 1.5 | 240.3 | 1.4 | 245.8 | 12.2 | 0.67 |
| 4 (L,el,23) | 0.0339 | 180.9 | 7.203 | 1440 | 10 | 0.53 | 0.03799 | 0.12 | 0.2678 | 0.34 | 0.05114 | 0.31 | 240.4 | 0.6 | 241.0 | 1.5 | 247.0 | 14.3 | 0.44 |
| 5 (M,eq,el,28) | 0.0110 | 207.7 | 8.438 | 1055 | 5 | 0.59 | 0.03809 | 0.16 | 0.2717 | 0.82 | 0.05174 | 0.78 | 241.0 | 0.8 | 244.1 | 3.6 | 273.8 | 36 | 0.37 |
| *F109* | | | | | | | | | | | | | | | | | | | |
| 1 (M,el,10) | 0.0203 | 375.8 | 15.48 | 2177 | 8 | 0.66 | 0.03799 | 0.16 | 0.2678 | 0.24 | 0.05112 | 0.16 | 240.4 | 0.8 | 241.0 | 1.0 | 246.5 | 7.3 | 0.74 |
| 2 (M,el,9) | 0.0167 | 311.1 | 12.61 | 1119 | 11 | 0.59 | 0.03798 | 0.22 | 0.2684 | 0.35 | 0.05125 | 0.26 | 240.3 | 1.0 | 241.4 | 1.5 | 252.3 | 11.9 | 0.67 |
| 3 (M,eq,17) | 0.0260 | 337.7 | 13.89 | 2919 | 7 | 0.63 | 0.03815 | 0.23 | 0.2684 | 0.25 | 0.05103 | 0.17 | 241.4 | 1.1 | 241.4 | 1.1 | 242.1 | 7.9 | 0.74 |
| 4 (M,eq,27) | 0.0317 | 403.4 | 16.53 | 4923 | 6 | 0.64 | 0.03793 | 0.13 | 0.2669 | 0.19 | 0.05103 | 0.16 | 240.0 | 0.6 | 240.2 | 0.8 | 242.1 | 7.4 | 0.57 |
| *Litér* | | | | | | | | | | | | | | | | | | | |
| 1 (S,n,12) | 0.0752 | 267.8 | 11.04 | 3777 | 13 | 0.57 | 0.03892 | 0.16 | 0.2790 | 0.17 | 0.05199 | 0.10 | 246.2 | 0.8 | 249.9 | 0.8 | 284.8 | 4.5 | 0.83 |
| 2 (L,eq,9) | 0.1249 | 164.8 | 6.478 | 1960 | 25 | 0.50 | 0.03779 | 0.35 | 0.2656 | 0.36 | 0.05097 | 0.13 | 239.1 | 1.7 | 239.2 | 1.5 | 239.5 | 5.8 | 0.94 |
| 3 (S,n,21) | 0.0555 | 330.2 | 13.46 | 4322 | 10 | 0.65 | 0.03769 | 0.14 | 0.2654 | 0.18 | 0.05106 | 0.12 | 238.5 | 0.6 | 239.0 | 0.8 | 243.6 | 5.3 | 0.77 |
| 4 (M,el,14) | 0.1249 | 254.6 | 10.63 | 9411 | 8 | 0.55 | 0.03953 | 0.23 | 0.2841 | 0.25 | 0.05212 | 0.12 | 249.9 | 1.1 | 253.9 | 1.1 | 290.7 | 5.3 | 0.88 |
| 5 (L,eq,t,24) | 0.1427 | 276.4 | 11.21 | 2057 | 45 | 0.54 | 0.03851 | 0.25 | 0.2746 | 0.28 | 0.05171 | 0.12 | 243.6 | 1.2 | 246.4 | 1.2 | 272.7 | 5.4 | 0.91 |

[1]All zircon fractions; size, morphology and number of grains are indicated in parentheses. S, smallest dimension of grain is <80 μm; M, >80 μm and <100 μm; L, >100 μm; eq, equant; el, elongate; n, needle-like; t, tabular.
[2]Radiogenic Pb.
[3]Measured ratio, corrected for spike and Pb fractionation (0.09% per a.m.u.).
[4]Total common Pb in analysis, corrected for fractionation and spike.
[5]Atomic ratio of Th to U, calculated from $^{208}Pb/^{206}Pb$.
[6]Corrected for blank Pb and U, and common Pb (Stacey–Kramers model Pb equivalent to interpreted age of mineral).
[7]Including decay constant uncertainty.

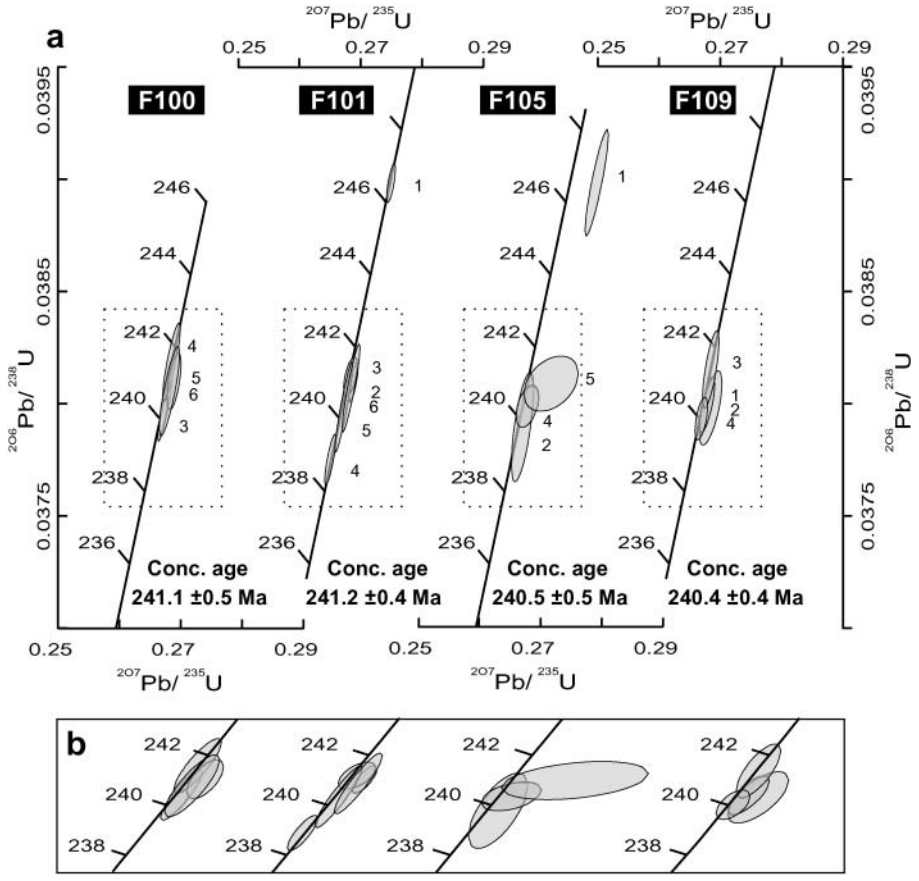


**Fig. 6.** Concordia diagram of zircons analysed from tuff samples from the Felsőörs section. Error ellipses shown at the 2$\sigma$ level, including decay constant errors. Insets marked by dashed line in (**a**) are enlarged on (**b**), to show the concordant and overlapping fractions that formed the basis of age interpretation.

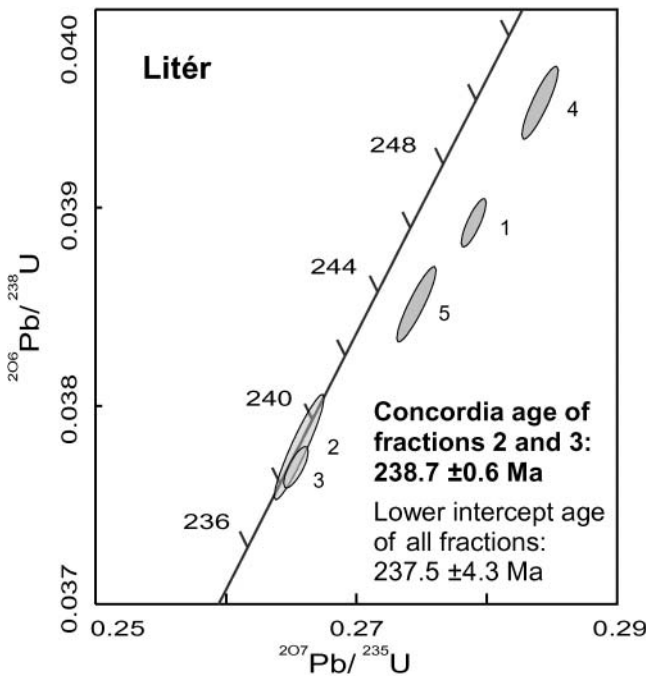


**Fig. 7.** Concordia diagram of zircons analysed from a tuff sample from the Litér quarry. Error ellipses shown at the 2$\sigma$ level, including decay constant errors.

at *c.* 239 Ma deviate from the remaining four fractions. Fraction 1 may be interpreted to contain one or more slightly older xenocrysts or grains with xenocryst cores, whereas the Pb loss suffered by fraction 4 was not entirely removed by the abrasion of grains. The other four fractions (2, 3, 5 and 6) are concordant and overlapping around a weighted mean $^{206}Pb/^{238}U$ age of 241.0 ± 0.4 Ma (Fig. 6). We use their concordia age of 241.2 ± 0.4 Ma as the best estimate of the crystallization age of the tuff.

*Sample F105.* Located 7 m stratigraphically above sample F101 in the Felsőörs section, this sample is derived from a 15 cm thick, brown weathering, coarse-grained, feldspar-rich crystal tuff. The sampled layer lies 45 cm above Bed 105, which contains limestone lenses that yielded *Reitziites reitzi* (Fig. 5c), *Parakellnerites* cf. *boeckhi* (Fig. 5e) and *Hungarites* sp. Bed 105 marks the base of the Reitzi Subzone of the Reitzi Zone in the section.

The sample yielded abundant, colourless zircons of excellent clarity and low U content (150–210 ppm). The morphology of euhedral grains is similar to that of the lower samples in the same section, ranging from doubly terminating prisms to needles of simple quadratic cross-section and length:width ratio up to 8:1. Of the four analysed fractions, three intersect the concordia curve and overlap one another, whereas fraction 1 is discordant, suggesting inheritance as a result of undetected cryptic cores or xenocrysts of older age. Fractions 2, 4 and 5 cluster around a weighted mean $^{206}Pb/^{238}U$ age of 240.5 ± 1.1 Ma (Fig. 6). We

**Table 2.** *Summary of age determinations*

| Sample | Locality | Ammonoid zone (subzone) | Fractions analysed | Concordant fractions* | Weighted mean $^{206}Pb/^{238}U$ age† | MSWD | Concordia age‡ | MSWD |
|---|---|---|---|---|---|---|---|---|
| F100 | Felsőörs | Reitzi (felsoeoersensis) | 6 | 4 | 241.0 ± 0.5 | 0.77 | 241.1 ± 0.5 | 1.5 |
| F101 | Felsőörs | Reitzi (liepoldti) | 6 | 4 | 241.0 ± 0.4 | 0.59 | 241.2 ± 0.4 | 3.4 |
| F105 | Felsőörs | Reitzi (reitzi) | 4 | 3 | 240.5 ± 1.1 | 1.4 | 240.5 ± 0.5 | 1.3 |
| F109 | Felsőörs | Reitzi (reitzi) | 4 | 4 | 240.3 ± 0.8 | 1.6 | 240.4 ± 0.5 | 2.4 |
| Litér | Litér | Gredleri | 5 | 2 | 238.6 ± 0.6 | 0.49 | 238.7 ± 0.6 | 1.4 |

*Used in age calculations.
†In Ma, with 2σ errors including decay constant uncertainty.
‡In Ma, with 2σ errors including decay constant uncertainty, calculated following the method of Ludwig (1998) using Isoplot v. 2.45 (Ludwig 2000).

use their concordia age of 240.5 ± 0.5 Ma as the best estimate of the crystallization age of the tuff.

*Sample F109*. The highest sample from the Felsőörs section was collected from a soft, green, 8 cm thick tuff layer. It underlies limestone Bed 109, which did not yield any ammonoids. Approximately 1.2 m higher, Beds 110 and 111 yielded *Latemarites latemarensis* (Fig. 5f–g), suggesting the base of the Avisianum Subzone. Therefore, sample F109 is interpreted to belong to the uppermost part of Reitzi Subzone within the Reitzi Zone.

The sample yielded abundant, pale brown zircons of excellent clarity. The U content (310–400 ppm) is somewhat higher than in the other samples from Felsőörs and zircon morphology is also slightly different. The euhedral grains represent a homogeneous population of simple, prismatic crystals with an aspect ratio of 3:1. All four analysed fractions intersect the concordia curve and overlap one another (Fig. 6), clustering around a weighted mean $^{206}Pb/^{238}U$ age of 240.3 ± 0.8 Ma. We use their concordia age of 240.4 ± 0.5 Ma as the best estimate of the crystallization age of the tuff.

*Sample Litér.* The sample was collected from the redeposited tuff filling a neptunian dyke in the SW wall of the Litér quarry. Internal moulds of ammonoids *Protrachyceras* cf. *gredleri* (Fig. 5h), *P.* cf. *longobardicum* (Fig. 5i), *Eoprotrachyceras*? cf. *pseudoarchelaus*, *Arpadites* cf. *arpadis* (Fig. 5j), *A*. aff. *arpadis* and *Proarcestes* cf. *subtridentinus* occur in the the same dyke fill, suggesting a maximum age of Gredleri Zone.

Abundant, colourless to pale yellow zircons of excellent clarity and low U content (160–330 ppm) were recovered from this sample. Simple, prismatic crystals with aspect ratio of 3:1 dominate the population, whereas elongated grains (length:width up to 6:1) are also common. Occasionally, cores were observed and those grains were excluded from the analyses. Nevertheless, three of the analysed five fractions are discordant, probably because of the presence of undetected cryptic cores or older xenocrysts. The discordant fractions loosely define a discordia line that, using all five fractions, points to a Proterozoic upper intercept age of 959 ± 320 Ma. Fractions 2 and 3 are concordant and overlap each other (Fig. 7), yielding a weighted mean $^{206}Pb/^{238}U$ age of 238.6 ± 0.6 Ma. It is nearly identical to their calculated concordia age of 238.7 ± 0.6 Ma, which is taken as the best estimate of the crystallization age of the tuff.

### *Synopsis of U–Pb dating*

The ages derived from the pooling of concordant data from each sample (noting the exclusion of two analyses of F101 as discussed above) yield the following ages: 241.1 ± 0.5 Ma, 241.2 ± 0.4 Ma, 240.5 ± 0.5 Ma, 240.4 ± 0.4 Ma and 238.7 ± 0.6 Ma for samples F100, F101, F105, F109 and Litér, respectively (Table 2). These are consistent with the biostratigraphic order of the samples. In this study we attempted to minimize the error arising from uncertainty in either the blank or common Pb composition correction. This necessitated the analysis of multiple grain fractions with very similar crystallographic and size characteristics. The ages reported in this paper are consistent with the single-grain analyses of Mundil *et al*. (1996) from comparable biostratigraphic horizons from the Southern Alps (Fig. 8). They used similar isotope dilution thermal ionization mass spectrometry analytical techniques, which included strong zircon air abrasion and leaching in warm weak $HNO_3$ but did not involve leaching in strong HF acid at elevated temperatures as in a more recent study by Mundil *et al*. (2001). The age of the sample from Litér is indistinguishable from the age obtained by Mundil *et al*. (1996) from a tuff at the same biostratigraphic level. The ages of the samples from Felsőörs are also unresolvable from two single-grain U–Pb ages from the next higher ammonoid zone in the Southern Alps (Mundil *et al*. 1996). This suggests the possibility of very minor but systematic unresolved Pb loss carried by one or more grains in all fractions (Mundil *et al*. 2001), that the Reitzi Zone was of short duration, or that the difference may relate in some subtle way to interlaboratory comparison of data. A follow-up study based on single-crystal analyses from the same tuff layers at Felsőörs will be useful to clarify if the single crystal v. multiple grain approaches to U–Pb dating yield identical results.

## Discussion

### *Implications for the Mid-Triassic time scale*

Combining our dataset with that of Mundil *et al*. (1996) makes the Mid-Triassic, and the Ladinian stage in particular, arguably the best calibrated part of the Triassic time scale (Fig. 8). Choosing the oldest option (base of Reitzi Zone) for the Anisian–Ladinian boundary results in a subdivision of the Ladinian stage into six ammonoid zones. The biostratigraphic position of dated tuffs is resolved to the subzone or zone level in the Balaton Highland, as reported here, and to the zone level in the Southern Alps (Mundil *et al*. 1996). Intervals with similar resolution in the Mesozoic time scale are still rare (Pálfy *et al*. 2000b), with the exception of the Late Cretaceous (Obradovich 1993). In the Ladinian, only the Curionii Zone lacks an isotopic date, if a U–Pb age of 237.3+0.4/−1.0 Ma of the Predazzo intrusion (Brack *et al*. 1997) is tentatively assigned to the Regoledanus Zone. The four dates from the Felsőörs section,

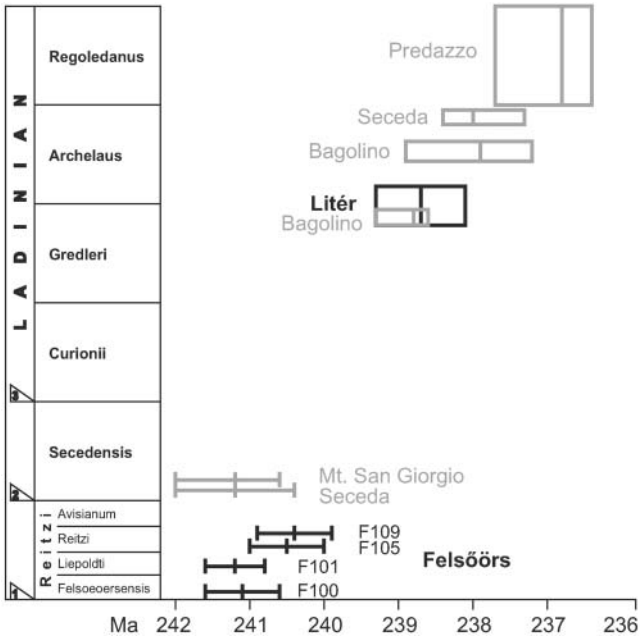


**Fig. 8.** Synopsis of Ladinian time scale calibration points using subzonally or zonally constrained U–Pb ages from the Balaton Highland (this study, marked by black bars) and the Southern Alps (marked by grey bars: Bagolino, Seceda and Monte San Giorgio from Mundil *et al*. (1996); Predazzo from Brack *et al*. (1997)). Formally proposed possible positions of the base of Ladinian are labelled 1, 2 and 3; preference in our dicussion is given to option 1. U–Pb ages are shown with 2$\sigma$ error bars; rectangles as opposed to bars denote uncertainty in the biostratigraphic position of dated rocks.

which span the lower three subzones of the Reitzi Zone, are overlapping, and are also statistically indistinguishable from the dates from the base of the overlying Secedensis Zone reported by Mundil *et al*. (1996). Considering their 2$\sigma$ errors, the maximum duration of the Reitzi Zone does not exceed 1.2 Ma. The good agreement between the dates of the upper Gredleri Zone from Litér (238.7 $\pm$ 0.6 Ma, this study) and Bagolino (238.8+0.5/−0.2 Ma, Mundil *et al*. 1996) argues against any significant systematic bias between the two datasets. The age of the lower and upper boundary of the Ladinian stage is estimated here at 241.5 and 237 Ma, respectively. Although this assessment lacks statistical rigour, it is based on a robust set of 11 U–Pb dates. Mundil *et al*. (1996) used a least-squares fit of their five dates normalized to the stratal thicknesses and biostratigraphy of the Bagolino reference section, but their estimate of 243.6 Ma for the base of Reitzi Zone appears too old if one considers the new dates, and the fitted curve does not permit a meaningful age estimation for the uppermost Ladinian.

As noted by Mundil *et al*. (1996), their U–Pb date from the base of Secedensis Zone at Monte San Giorgio supersedes the $^{40}Ar/^{39}Ar$ age of 233 $\pm$ 7 Ma obtained by Hellmann & Lippolt (1981), which was used as a key tie-point in several recently published time scales. Thus the Anisian–Ladinian boundary was estimated at 234.3 $\pm$ 4.6 Ma by Gradstein *et al*. (1994) and 233 $\pm$ 5 Ma by Odin (1994) and Remane (2000). The duration of the Ladinian is estimated here as 4.5 Ma, 50% less than the value given by Gradstein *et al*. (1994) and 50% more than that of Odin (1994) and Remane (2000). The closest agreement exists, perhaps fortuitously, with the time scale of Harland *et al*. (1990), which quotes an Anisian–Ladinian boundary age of 239.5 Ma and estimates the duration of the Ladinian at 4.5 Ma.

### *Implications for calibrating cyclostratigraphies*

Our dating results bear on a controversy over the cyclicity of the Ladinian Latemar platform in the Dolomites. During Mid-Triassic time, large tracts of the western Tethyan continental margin were characterized by growth of carbonate platforms and pelagic sedimentation in intervening basins. Reconstructions for our study area also propose a palaeogeographical model of alternating platforms and basins (Vörös *et al*. 1997; Budai *et al*. 2001a), but more extensively studied are the spectacularly developed, coeval carbonate platforms in the Southern Alps, especially in the Dolomites. The Latemar platform is a 720 m thick buildup of cyclic limestone that was interpreted to express eccentricity-modulated precession cycles (Goldhammer *et al*. 1987; Hinnov & Goldhammer 1991). Assuming Milankovitch forcing, the deposition of 600 cycles observed in the inner platform required 12 Ma. More detailed spectral analysis of part of the cyclic facies appears to confirm its orbital tuning, thus the Latemar has been proposed to preserve the oldest known pristine Milankovitch signature in the geological record (Preto *et al*. 2001). Yet this view is not universally accepted and Milankovitch forcing of the Latemar was partly or entirely discounted on the basis of earlier U–Pb dating. Findings of ammonoids and the thin-shelled bivalve *Daonella* constrain the platform growth to within the Reitzi Zone (Avisianum Subzone) to the Gredleri Zone (Brack *et al*. 1996), an interval of less than 5 Ma as shown by the U–Pb dates of Mundil *et al*. (1996). Recently found ammonoids near the top of the Latemar platform suggest an even more restricted life span of the platform up to the Curionii Zone, or an equivalent of 4 Ma according to the same U–Pb dataset. For comparison, the growth period of the neighbouring Rosengarten platform spanned the interval of Reitzi to Archelaus zones (Maurer 2000).

The U–Pb dates presented here are relevant to this controversy in that they also bracket the conservatively estimated growth interval of the Latemar platform, i.e. the Reitzi to Gredleri zones. Considering the uncertainties, this time span is estimated as no more than 3.8 Ma, i.e. the difference between the age of samples F109 and Litér. These values are slightly lower than those of Mundil *et al*. (1996), who calculated a maximum of 4.7 Ma. Both studies conclude that this interval is significantly shorter than the 12 Ma as suggested by precession-based cyclostratigraphy. Thus the discrepancy between the Milankovitch and the isotopic time scales remains, although this study adds weight to the arguments in favour of the isotopic time scale. Accepting the time constraints derived from these U–Pb ages, the principal tuning parameter of the Latemar depositional cycles must be in the sub-Milankovitch band, rather than the orbital precession of 20 ka frequency. A further test of cyclostratigraphy is expected through continuing studies of correlative basinal strata recovered from the Seceda drill core (Brack *et al*. 2000).

### *Implications for rates of evolution after the latest-Permian extinction*

Assessing rates of biotic evolution is a research goal that requires an accurately calibrated, high-resolution time scale. The Ladinian time scale constructed here is useful for measuring the evolutionary tempo in Mid-Triassic time, an interval of diversification after the latest-Permian mass extinction. The Permian–Triassic boundary is marked by the most severe crisis in the history of life, which eliminated an estimated 95% of all marine species (Sepkoski 1996). The age of this boundary is defined by dating volcanic ash beds in South China, most notably from the

Meishan section, which contains the basal Triassic GSSP. Volcaniclastic layers very near the system boundary yielded an $^{40}Ar/^{39}Ar$ age of $250.0 \pm 3.6$ Ma (including decay constant uncertainty) (Renne *et al*. 1995, 1998), a sensitive high-resolution ion microprobe U–Pb age of $251.1 \pm 3.4$ Ma (Claoué-Long *et al*. 1991), a suite of conventional U–Pb ages using air-abraded single zircons and multi-grain fractions, including an age of $251.4 \pm 0.3$ Ma from the ash closest to the boundary bed (Bowring *et al*. 1998), and a suite of conventional U–Pb ages on HF-leached single zircons, implying an age >254 Ma for the same tuff below the boundary and $252.5 \pm 0.3$ Ma for another layer immediately above (Mundil *et al*. 2001). Taken together with our estimate of 241.5 Ma for the Anisian–Ladinian boundary, this dataset suggests that the Ladinian started *c*. 10 Ma after the Permian–Triassic boundary.

Palaeontological data for several fossil groups indicate that Early and Mid-Triassic times were characterized by successive intervals of survival, recovery and radiation. Fossil reefs, which harbour much of the marine biodiversity, were virtually wiped out at the end of Permian time, the tropical reef zone was severely constricted (Kiessling 2001), and the reef ecosystem was not re-established until Mid-Triassic time, with only small build-ups recorded in the Anisian period (Stanley 1988). A similarly long lag phase was noted in equatorial forests, a key component in terrestrial ecosystems, throughout almost the whole of Early Triassic time, and the Permian and later Triassic proliferation of conifers was replaced by a temporary dominance of bryophytes and lycopsids (Looy *et al*. 1999).

The rebound of ammonoids started somewhat earlier in Early Triassic time, but was interrupted by a smaller extinction at the Early–Mid-Triassic boundary (Tozer 1981). The Anisian and Ladinian are times of diversification, although high origination rates are offset by elevated extinction rates. The resulting high turnover underpins the high biostratigraphic resolution, which is numerically calibrated here. The Ladinian, which comprises six zones, is estimated to have a duration of 4.5 Ma, which translates to an average zonal duration of 0.75 Ma. Our data permit even shorter durations (a few hundred ka) for the Reitzi and Secedensis zones. This interval might represent a peak in evolutionary rate, although this claim cannot be substantiated until the earlier Triassic time scale is similarly resolved to the zone level. The length of the Anisian period remains poorly constrained, but our data are consistent with a prolonged Early Triassic interval of suppressed diversity followed by a somewhat shorter, rapid burst of evolution in Mid-Triassic time, thus supporting logistic models of post-extinction diversification (Erwin 1998; Eble 1999). It is interesting to note that although the Early Triassic recovery is widely assumed to be more protracted than others, a cross-correlation analysis of extinctions and originations in the entire fossil record detects a typical 10 Ma time lag in biotic recoveries (Kirchner & Weil 2000). Our further studies will attempt to obtain calibration points for the older part of the Triassic and to use this time frame in quantifying Triassic evolutionary rates.

## Conclusions

Five new zircon U–Pb ages contribute to the calibration of the Ladinian time scale at the biozone and subzone level. Four isotopic dates are integrated with ammonoid biostratigraphy from the Reitzi Zone (in our view, basal Ladinian) in the Felsőörs section, a candidate for the Anisian–Ladinian boundary stratotype (GSSP). A tuff layer in the Felsoeoersensis Subzone is dated as $241.1 \pm 0.5$ Ma, one in the Liepoldti Subzone is dated as $241.2 \pm 0.4$ Ma, and two tuffs in the Reitzi Subzone yielded ages of $240.5 \pm 0.5$ and $240.4 \pm 0.4$ Ma. An additional date of $238.7 \pm 0.6$ Ma is obtained from the Gredleri Zone at Litér. These results are in good agreement with a set of U–Pb dates reported by Mundil *et al*. (1996) from the Southern Alps. Taken together, they permit an estimate of 241.5 and 237 Ma for the beginning and the end of the Ladinian stage, respectively. Zonal duration varied within the 4.5 Ma Ladinian; the oldest Reitzi and Secedensis zones were probably among the shorter ones with a length of only a few hundred ka. Empirically established, short ammonoid zones reflect an elevated evolutionary turnover rate, suggesting that Mid-Triassic time was a period of rapid diversification following an extended period of low diversity in Early Triassic time, after the latest-Permian mass extinction.

This dataset can be used to assess the controversial forcing of cyclic deposits of the Latemar platform in the Southern Alps. Our dates from the Reitzi and Gredleri zones constrain the growth period of the Latemar buildup to less than 3.8 Ma. This is in agreement with findings of Mundil *et al*. (1996) but such an isotopic time scale remains at variance with Milankovitch-based estimates (Goldhammer *et al*. 1987; Hinnov & Goldhammer 1991; Preto *et al*. 2001) that suggest a substantially longer time frame. Now two independent suites of U–Pb ages from different geographical localities and different laboratories imply that at least some of the allocyclic processes recorded in the Latemar platform operated at sub-Milankovitch time scales.

We are grateful to I. Szabó for help in collecting ammonoids, and to T. Budai, L. Hinnov and R. Mundil for helpful discussions. L. Krystyn donated ammonoids collected from the Felsőörs section and allowed A.V. to study his collections from Epidaurus. Journal reviews by R. Mundil, P. Cawood and R. A. Cliff helped improved the manuscript. This research was supported through grants from the Hungarian Scientific Research Fund (OTKA T29965 and T26278), the Natural Environment Research Council (UK), the British Council, and a British–Hungarian Science and Technology Co-operation Grant. J.P. acknowledges support from a Bolyai Research Fellowship.

## References

Balini, M., Germani, D., Nicora, A. & Rizzi, E. 2000. Ladinian/Carnian ammonoids and conodonts from the classic Schilpario–Pizzo Camino area (Lombardy): reevaluation of the biostratigraphic support to chronostratigraphy and paleogeography. *Rivista Italiana di Paleontologia e Stratigrafia*, **106**, 19–58.

Balogh, K. 1981. Correlation of the Hungarian Triassic. *Acta Geologica Hungarica*, **24**, 3–48.

Böckh, J. 1873. Die geologischen Verhältnisse des südlichen Theiles des Bakony, I. *Mittheilungen aus dem Jahrbuche der Königlichen Ungarischen Geologischen Anstalt*, **2**, 27–182.

Bowring, S.A., Erwin, D.H., Jin, Z.G., Martin, M.W., Davidek, K. & Wang, W. 1998. U/Pb zircon geochronology and tempo of the end-Permian mass extinction. *Science*, **280**, 1039–1045.

Brack, P. & Rieber, H. 1993. Towards a better definition of the Anisian/Ladinian boundary: new biostratigraphic data and correlations of boundary sections from the Southern Alps. *Eclogae Geologicae Helvetiae*, **86**, 415–527.

Brack, P. & Rieber, H. 1994. The Anisian/Ladinian boundary: retrospective and new constraints. *Albertiana*, **13**, 25–36.

Brack, P., Mundil, R., Oberli, F., Meier, M. & Rieber, H. 1996. Biostratigraphic and radiometric age data question the Milankovitch characteristics of the Latemar cycles (Southern Alps, Italy). *Geology*, **24**, 371–375.

Brack, P., Mundil, R., Oberli, F., Meier, M. & Rieber, H. 1997. Biostratigraphic and radiometric age data question the Milankovitch characteristics of the Latemar cycles (Southern Alps, Italy): reply. *Geology*, **25**, 471–472.

Brack, P., Schlager, W., Stefani, M., Maurer, F. & Kenter, J. 2000. The Seceda boring in the Middle Triassic Buchenstein beds (Livinallongo Formation,Dolomites, Northern Italy)—a progress report. *Rivista Italiana di Paleontologia e Stratigrafia*, **106**, 283–292.

Budai, T. 1992. Middle Triassic formations of the Balaton Highland and of the Southern Alps: stratigraphic correlation. *Acta Geologica Hungarica*, **35**, 217–236.

Budai, T. & Vörös, A. 1992. Middle Triassic history of the Balaton Highland: extensional tectonics and basin evolution. *Acta Geologica Hungarica*, **35**, 237–250.

Budai, T. & Vörös, A. 1993. The Middle Triassic events of the Transdanubian Central Range in the frame of the Alpine evolution. *Acta Geologica Hungarica*, **36**, 3–13.

Budai, T., Csillag, G., Vörös, A. & Dosztály, L. 2001*a*. Middle to Late Triassic platform and basin facies of the Veszprém Plateau (Transdanubian Range, Hungary). *Földtani Közlöny (Bulletin of the Hungarian Geological Society)*, **131**, 37–70 (in Hungarian).

Budai, T., Csillag, G., Vörös, A. & Lelkes, G. 2001*b*. Middle to Late Triassic platform and basin facies of the Eastern Bakony Mts. (Transdanubian Range, Hungary). *Földtani Közlöny (Bulletin of the Hungarian Geological Society)*, **131**, 71–95 (in Hungarian).

Castellarin, A., Lucchini, F., Rossi, P.L., Simboli, G., Bosellini, A. & Sommavilla, E. 1980. Middle Triassic magmatism in the Southern Alps II: a geodynamic model. *Rivista Italiana di Paleontologia e Stratigrafia*, **85**, 1111–1124.

Claoué-Long, J.C., Zichao, Z., Gougan, M. & Shaohua, D. 1991. The age of the Permian–Triassic boundary. *Earth and Planetary Science Letters*, **105**, 182–190.

Cros, P. & Szabó, I. 1984. Comparison of the Triassic volcanogenic formations in Hungary and in the Alps. Paleogeographic criteria. *Acta Geologica Hungarica*, **27**, 265–276.

De Zanche, V., Gianolla, P., Manfrin, S., Mietto, P. & Roghi, G. 1995. A Middle Triassic back-stepping carbonate platform in the Dolomites (Italy): sequence stratigraphy and biochronostratigraphy. *Memorie di Scienze Geologiche*, **47**, 135–155.

Dunkl, I. 1992. Origin of Eocene-covered karst bauxites of the Transdanubian Central Range (Hungary): evidence for early Eocene volcanism. *European Journal of Mineralogy*, **4**, 581–595.

Eble, G.J. 1999. Originations—land and sea compared. *Geobios*, **32**, 223–234.

Erwin, D.H. 1998. The end and the beginning: recoveries from mass extinctions. *Trends in Ecology and Evolution*, **13**, 344–349.

Fantini Sestini, N. 1994. The Ladinian ammonoids from Calcare di Esino of Val Parina (Bergamasc Alps, Northern Italy). Pt. 1. *Rivista Italiana di Paleontologia e Stratigrafia*, **100**, 227–284.

Goldhammer, R.K., Dunn, P.A. & Hardie, L.A. 1987. High frequency glacio-eustatic sea level oscillactions with Milankovitch characteristics recorded in Middle Triassic platform carbonates in northern Italy. *American Journal of Science*, **287**, 853–892.

Gradstein, F.M., Agterberg, F.P., Ogg, J.G., Hardenbol, J., van Veen, P., Thierry, J. & Huang, Z. 1994. A Mesozoic time scale. *Journal of Geophysical Research,* **B99**, 24051–24074.

Haas, J. & Budai, T. 1995. Upper Permian–Triassic facies zones in the Transdanubian Range. *Rivista Italiana di Paleontologia e Stratigrafia*, **101**, 249–266.

Haas, J. & Budai, T. 1999. Triassic sequence stratigraphy of the Transdanubian Range (Hungary). *Geologica Carpathica*, **50**, 459–475.

Haas, J., Kovács, S., Krystyn, L. & Lein, R. 1995. Significance of Late Permian–Triassic facies zones in terrane reconstructions in the Alpine North Pannonian domain. *Tectonophysics*, **242**, 19–40.

Hardie, L.A. & Hinnov, L. 1997. Biostratigraphic and radiometric age data question the Milankovitch characteristics of the Latemar cycles (Southern Alps, Italy): comment. *Geology*, **25**, 470–471.

Harland, W.B., Armstrong, R.L., Cox, A.V., Craig, L.E., Smith, A.G. & Smith, D.G. 1990. *A Geologic Time Scale 1989*. Cambridge University Press, Cambridge.

Hellmann, K.N. & Lippolt, H.J. 1981. Calibration of the Middle Triassic time scale by conventional K–Ar and $^{40}Ar/^{39}Ar$ dating of alkali feldspars. *Journal of Geophysics*, **50**, 73–86.

Hinnov, L. & Goldhammer, R.K. 1991. Spectral analysis of the Middle Triassic Latemar Limestone. *Journal of Sedimentary Petrology*, **61**, 1173–1193.

Jaffey, A.H., Flynn, K.F., Glendenin, L.E., Bentley, W.C. & Essling, A.M. 1971. Precision measurements of half-lives and specific activities of $^{235}U$ and $^{238}U$. *Physical Reviews*, **C4**, 1889–1906.

Kázmér, M. & Kovács, S. 1985. Permian–Paleogene paleogeography along the eastern part of the Insubric–Periadriatic lineament system. Evidence for continental escape of the Bakony–Drauzug Unit. *Acta Geologica Hungarica*, **28**, 71–84.

Kiessling, W. 2001. Paleoclimatic significance of Phanerozoic reefs. *Geology*, **29**, 751–754.

Kirchner, J.W. & Weil, A. 2000. Delayed biological recovery from extinctions throughout the fossil record. *Nature*, **404**, 177–180.

Kovács, S. 1993. Conodont biostratigraphy of the Anisian/Ladinian boundary interval in the Balaton Highland, Hungary and its significance in the definition of the boundary (Preliminary report). *Acta Geologica Hungarica*, **36**, 39–57.

Kovács, S., Szederkényi, T., Haas, J., Buda, G., Császár, G. & Nagymarosy, A. 2000. Tectonostratigraphic terranes in the pre-Neogene basement of the Hungarian part of the Pannonian area. *Acta Geologica Hungarica*, **43**, 225–328.

Kozur, H., Mock, R. & Ozvoldová, L. 1995. The age of red radiolarites from the Meliaticum of Bohunovo (Slovakia) and remarks to the Anisian–Ladinian boundary. *Mineralia Slovaca*, **27**, 153–168.

Krogh, T.E. 1982. Improved accuracy of U–Pb zircon ages by the creation of more concordant systems using an air abrasion technique. *Geochimica et Cosmochimica Acta*, **46**, 637–649.

Krystyn, L. 1983. Das Epidaurus-Profil (Griechenland)—ein Beitrag zur Conodonten-Standardzonierung der tethyalen Ladin und Unterkarn. *In:* Zapfe, H. (ed.) *Neue Beiträge zur Biostratigraphie der Tethys–Trias*. Schriftenreihe der Erdwissenschaftlichen Kommissionen, Österreichische Akademie der Wissenschaften, Wien, **5**, 231–258.

Looy, C., Brugman, W., Dilcher, D. & Visscher, H. 1999. The delayed resurgence of equatorial forests after the Permian–Triassic ecologic crisis. *Proceedings of the National Academy of Sciences, USA*, **96**, 13597–13599.

Ludwig, K.R. 1998. On the treatment of concordant uranium–lead ages. *Geochimica et Cosmochimica Acta*, **62**, 665–676.

Ludwig, K.R. 2000. *Isoplot/Ex 2.45, A Geochronological Toolkit for Microsoft Excel*. Berkeley Geochronology Center, Berkeley, CA.

Márton, E., Budai, T., Haas, J., Kovács, J., Szabó, I. & Vörös, A. 1997. Magnetostratigraphy and biostratigraphy of the Anisian–Ladinian boundary section Felsőörs (Balaton Highland, Hungary). *Albertiana*, **20**, 50–57.

Maurer, F. 2000. Growth mode of Middle Triassic carbonate platforms in the Western Dolomites (Southern Alps Italy). *Sedimentary Geology*, **134**, 275–286.

Mietto, P. & Manfrin, S. 1995. A high resolution Middle Triassic ammonoid standard scale in the Tethys Realm. A preliminary report. *Bulletin de la Société Géologique de France*, **166**, 539–563.

Mojsisovics, E. 1882. Die Cephalopoden der mediterranen Triasprovinz. *Abhandlungen der Kaiserlich–Königlichen Geologischen Reichanstalt*, **10**, 1–322.

Mundil, R., Brack, P., Meier, M., Rieber, H. & Oberli, F. 1996. High resolution U–Pb dating of Middle Triassic volcaniclastics: time-scale calibration and verification of tuning parameters for carbonate sedimentation. *Earth and Planetary Science Letters*, **141**, 137–151.

Mundil, R., Metcalfe, I., Ludwig, K.R., Renne, P.R., Oberli, F. & Nicoll, R.S. 2001. Timing of the Permian–Triassic biotic crisis: implications from new zircon U/Pb age data (and their limitations). *Earth and Planetary Science Letters*, **187**, 131–145.

Noble, S.R., Tucker, T.C. & Pharaoh, T.C. 1993. Lower Palaeozoic and Precambrian igneous rocks from eastern England, and their bearing on late Ordovician closure of the Tornquist Sea: constraints from U–Pb and Nd isotopes. *Geological Magazine*, **130**, 835–846.

Obradovich, J.D. 1993. A Cretaceous time scale. *In:* Caldwell, W.G.E. & Kauffman, E.G. (eds) *Evolution of the Western Interior Basin*. Geological Association of Canada Special Paper, **39**, 379–396.

Odin, G.S. 1994. Geological time scale. *Comptes Rendus de l'Académie des Sciences, Série II*, **318**, 59–71.

Pálfy, J. & Vörös, A. 1998. Quantitative ammonoid biochronological assessment of the Anisian–Ladinian (Middle Triassic) stage boundary proposals. *Albertiana*, **21**, 19–26.

Pálfy, J., Mortensen, J.K., Carter, E.S., Smith, P.L., Friedman, R.M. & Tipper, H.W. 2000a. Timing the end-Triassic mass extinction: first on land, then in the sea? *Geology*, **28**, 39–42.

Pálfy, J., Smith, P.L. & Mortensen, J.K. 2000b. A U–Pb and $^{40}Ar/^{39}Ar$ time scale for the Jurassic. *Canadian Journal of Earth Sciences*, **37**, 923–944.

Parrish, R.R. 1987. An improved micro-capsule for zircon dissolution in U–Pb geochronology. *Chemical Geology (Isotope Geoscience Section)*, **66**, 99–102.

Parrish, R.R., Roddick, J.C., Loveridge, W.D. & Sullivan, R.W. 1987. Uranium–lead analytical techniques at the geochronology laboratory. *Geological Survey of Canada, Paper*, 3–7.

Pisa, G., Castellarin, A., Lucchini, F., Rossi, P.L., Simboli, G., Bosellini, A. & Sommavilla, E. 1980. Middle Triassic magmatism in the Southern Alps. I: A review of general data in the Dolomites. *Rivista Italiana di Paleontologia e Stratigrafia*, **85**, 1093–1110.

Preto, N., Hinnov, L.A., Hardie, L.A. & De Zanche, V. 2001. Middle Triassic orbital signature recorded in the shallow-marine Latemar carbonate buildup (Dolomites, Italy). *Geology*, **29**, 1123–1126.

Remane, J. 2000. *International Stratigraphic Chart*. International Union of Geological Sciences, Paris.

Renne, P.R., Zichao, Z., Richards, M.A., Black, M.T. & Basu, A.R. 1995. Synchrony and causal relations between Permian–Triassic boundary crises and Siberian flood volcanism. *Science*, **269**, 1413–1416.

Renne, P.R., Swisher, C.C., Deino, A.L., Karner, D.B., Owens, T.L. & DePaolo, D.J. 1998. Intercalibration of standards, absolute ages an uncertainties in $^{40}Ar/^{39}Ar$ dating. *Chemical Geology*, **145**, 117–152.

Roddick, J.C. 1987. Generalized numerical error analysis with applications to geochronology and thermodynamics. *Geochimica et Cosmochimica Acta*, **51**, 2129–2135.

Roth, L. 1871. The geological cross-section of the slope of Forrás Hill at Felsőörs. *Földtani Közlöny (Bulletin of the Hungarian Geological Society)*, **1**, 209–215 (in Hungarian).

Schwarzacher, W. 1998. Bed thickness measurements and the cyclostratigraphy of the Latemar Limestone. *15th International Sedimentological Congress, Alicante*. Universidad di Alicante, 707.

Sepkoski, J.J. Jr 1996. Patterns of Phanerozoic extinction: a perspective from global data bases. *In:* Walliser, O.H. (ed.) *Global Events and Event Stratigraphy in the Phanerozoic*. Springer, Berlin, 35–51.

Stacey, J.S. & Kramers, J.D. 1975. Approximation of terrestrial lead isotope evolution by a two-stage model. *Earth and Planetary Science Letters*, **26**, 207–221.

Stanley, G.D. 1988. The history of early Mesozoic reef communities: a three step process. *Palaios*, **3**, 170–183.

Steiger, R.H. & Jäger, E. 1977. Subcommission on geochronology: convention on the use of decay constants in geo- and cosmochronology. *Earth and Planetary Science Letters*, **36**, 359–362.

Stürzenbaum, J. 1875. Data to the knowledge of the fauna of the Ceratites Reitzi-horizon from the Bakony. *Földtani Közlöny (Bulletin of the Hungarian Geological Society)*, **5**, 253–262 [in Hungarian].

Szabó, I., Kovács, S., Lelkes, G. & Oravecz-Scheffer, A. 1980. Stratigraphic investigation of a Pelsonian–Fassanian section at Felsőörs (Balaton Highland, Hungary). *Rivista Italiana di Paleontologia e Stratigrafia*, **85**, 789–806.

Tozer, E.T. 1981. Triassic Ammonoidea: classification, evolution, and relationship with Permian and Jurassic forms. *In:* House, M.R. & Senior, J.R. (eds) *The Ammonoidea*. Systematics Association Special Publication, **18**, 46–100.

Vörös, A. 1993. Redefinition of the Reitzi Zone at its type region (Balaton area, Hungary) as the basal zone of the Ladinian. *Acta Geologica Hungarica*, **36**, 15–38.

Vörös, A. 1998. Triassic ammonoids and biostratigraphy of the Balaton Highland. *Studia Naturalia*, **12**, 1–105 [in Hungarian].

Vörös, A. 2000. The Triassic of the Alps and Carpathians and its interregional correlation. *In:* Yin, H., Dickins, J.M., Shi, G.R. & Tong, J. (eds) *Permian–Triassic Evolution of Tethys and Western Circum-Pacific*. Elsevier, Amsterdam, 173–196.

Vörös, A. & Galácz, A. 1998. Jurassic palaeogeography of the Transdanubian Central Range (Hungary). *Revista Italiana di Paleontologia e Stratigrafia*, **104**, 69–84.

Vörös, A., Szabó, I., Kovács, S., Dosztály, L. & Budai, T. 1996. The Felsőörs section: a possible stratotype for the base of the Ladinian stage. *Albertiana*, **17**, 25–40.

Vörös, A., Budai, T., Lelkes, G., Monostori, M. & Pálfy, J. 1997. Middle Triassic basin evolution of the Balaton Highland (Hungary) based on sedimentological and paleoecological studies. *Földtani Közlöny (Bulletin of the Hungarian Geological Society)*, **127**, 145–177 [in Hungarian].

Received 28 February 2002; revised typescript accepted 25 October 2002.
Scientific editing by Jane Francis